Molecular Crystals and Liquid Crystals

Publication details, including instructions for authors and subscription information:
http://www.tandfonline.com/loi/gmcl20

2-Halooxyethylene ethers of cholesterol as novel single component, room temperature cholesteric LC materials

Santanu Bhattacharya [a] & Yamuna Krishnan-Ghosh [a]

[a] Department of Organic Chemistry, Indian Institute of Science, Bangalore, 560 012, India

Version of record first published: 18 Oct 2010

To cite this article: Santanu Bhattacharya & Yamuna Krishnan-Ghosh (2002): 2-Halooxyethylene ethers of cholesterol as novel single component, room temperature cholesteric LC materials, Molecular Crystals and Liquid Crystals, 381:1, 33-41

To link to this article: http://dx.doi.org/10.1080/713738738

Mol. Cryst. Liq. Cryst., Vol. 381, pp. 33–41

1058-725X/02 $12.00 + .00
DOI: 10.1080/10587250290102080

2-HALOOXYETHYLENE ETHERS OF CHOLESTEROL AS NOVEL SINGLE COMPONENT, ROOM TEMPERATURE CHOLESTERIC LC MATERIALS

Santanu Bhattacharya and Yamuna Krishnan-Ghosh*
Department of Organic Chemistry, Indian Institute of Science, Bangalore 560 012, India

A series of 2-haloethoxyethyl cholesteryl ethers has been synthesized. Each material shows attractive liquid-crystalline properties as revealed by differential scanning calorimetry, polarizing microscopy, and temperature-dependence of selective reflection characteristic of the cholesteric mesophase. These are interesting examples of simple, nonpolymeric, single component systems that show the cholesteric mesophase at room temperature.

Keywords: cholesterics; room temperature mesophase; single component LC; selective reflection

When light is incident on a cholesteric liquid crystal (LC) in the planar texture, reflection of light of a preferred wavelength occurs [1]. This property has resulted in thermotropic cholesterics being utilized in circular polarizers, bandpass filters, notch filters, pigments, and wide band reflective polarizers [2]. Although virtually all commercial liquid crystal displays (LCDs) today are based on twisted nematics [3] or supertwisted nematics [4], recent developments have shown that cholesteric LCD projection optics are more compact, and since they Bragg reflect light, these are brighter. This has spurred interest in the design of new cholesteric materials in order to develop the cholesteric optical concept [5]. Currently the field is dominated by polymers which form a minority of cholesteric materials, such as polymer dispersed liquid crystals [6], polyimides [7], LC gels [8], polymer-filled nematics [9], cellulose derivatives, etc. [10]. However, an inconvenience that persists in the application of cholesteric

Received 21 September 2001; accepted 24 February 2002.

This work was supported by the Swarnajayanti Fellowship awarded to SB by the Department of Science and Technology, Government of India.

*Corresponding author. Fax: +91-80-360-0529, E-mail: sb@orgchem.iisc.ernet.in; also at the Chemical Biology Unit of JNCASR, Bangalore 560 012, India.

materials is the formation of the LC phase only at elevated temperatures. Few monomer systems that are based on cholesteryl esters, carbonates, or urethanes exhibit the cholesteric mesophase at ambient temperatures [11]. However, mixtures of monomeric systems exhibit ambient temperature mesophases [12]. Thus cholesteric LCs used in LCDs are usually mixtures of chiral dopants in nematic LCs, typically biphenyl or terphenyl compounds with cyano or alkyl substituents [13]. One of the main applications of cholesteric LCs is as a temperature indicator [14]. As the pitch of the helix (p) varies with temperature, the wavelength of light that is reflected correspondingly changes. This thermochromic behavior associated with cholesteric LCs in the planar texture has resulted in their use as thermometers for a wide range of applications, ranging from diagnosing tumors in the human body to detecting shorts in electric circuit boards [15].

In the course of our investigations on the design of novel cholesterol-derived amphiphiles for various biological and materials applications [16] we recently synthesized several cholesterol derivatives based on hydrolytically stable ether linkages. During these studies, we serendipitously encountered a group of ether-linked ω-haloethoxy-ethanol derivatives of cholesterol, **1a**–**c**, that shows impressive LC properties at room temperature (Figure 1). In their mesophase regimes, **1a**–**c** display iridescent colors spanning the whole visible region. The colors of films of **1a**–**c** are quickly and reversibly modulated to reflect selected wavelengths by change in temperature. These compounds **1a**–**c** were obtained[1] as iridescent melts at room temperature, forming isotropic melts beyond $\sim 45^{\circ}$C. Upon cooling below the temperature regimes indicated in Table 1, these could be converted into smectic A phases.

When sandwiched between two glass plates, the compounds **1a**–**c** in their cholesteric phase show typical iridescent colors ranging from greenish-blue at higher temperatures to red at lower temperatures (Figure 2).

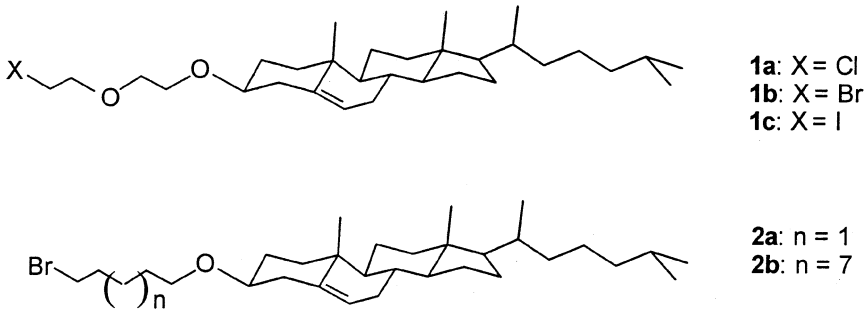

FIGURE 1 Molecular structures of the liquid crystals investigated herein.

TABLE 1 Thermodynamic Parameters for the Phase[a] Transitions of Liquid Crystals **1a**–**c** as Determined by DSC

	Phase transition temperature[b](°C) and corresponding ΔH (kJ/mol)[c]	
Compound	Heating	Cooling
1a	[d]Cryst. 39.2 (3.26) N* 46.0 (0.42) I Sm_A 22.8 (0.44) N* 45.3 (0.42) I	I 45.5 (0.42) N* 21.9(0.41) Sm_A
1b	[d]Cryst. 39.8 (20.9) N* 46.5 (0.43) I Sm_A 16.7 (0.42) N* 46.5 (0.42) I	I 46.4 (0.42) N* 16.1 (0.4) Sm_A
1c	[d]Cryst. 41.1 (26.4) N* 49.5 (1.26) I Sm_A 24.2 (0.42) N* 49.1 (1.26) I	I 48.9 (2.09) N* 24.2 (0.42) Sm_A
2a	[d]Cryst. 63.3 (18.41) N* 66.8 (0.42) I	I 65.6[e](−) broad trans. (8.37)[f] Cryst
2b	[d]Cryst. 72.7[e] (−) N* 75.2 (22.59)[f] I	I 59.8[e] (−) N* 58.9 (0.42)[f] Sm_A

[a]Cryst = crystal; N* = chiral nematic (cholesteric); Sm_A = smectic A; I, isotropic liquid.

[b]Transition temperatures as determined using a variable temperature polarizing microscope were within ± 1°C.

[c]Enthalpies of the transitions are given in parenthesis. Except for the first heating scans, the enthalpies and temperatures are the averages of three successive runs.

[d]First heating endotherm of the solid mass. The cooling curve was identical in all scans. All the subsequent heating endotherms were identical to the second heating endotherm reported on the second line.

[e]Peaks were too close to be resolved.

[f]Since the individual transition enthalpies could not determined accurately due to closeness of the transitions, the total enthalpy is reported in parentheses.

The colors are stable for several months at room temperature. In order to obtain precise information regarding the dependence of the wavelength that is selectively reflected (λ_{max}) with temperature (T) a thin film (~10 μm thickness) of each of **1a**–**c** was sandwiched between two quartz plates. The UV-Vis spectra (Shimadzu UV-2100 spectrophotometer) of these samples were then examined at different temperatures. Thin cholesteric films were produced by allowing the sample to incubate above the Sm_A-to-N* phase transition for 4 h on an individual quartz plate and

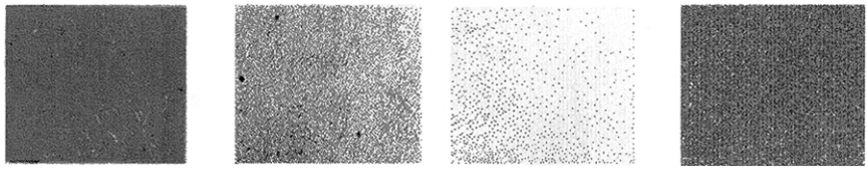

FIGURE 2 Photographs of solid cholesteric films (10 μm thickness) of **1b** at four different temperatures showing change in the wavelength of reflection. **A**, at 46°C; **B**, at 34°C; **C**, at 26.5°C; **D**, at 17.5°C.

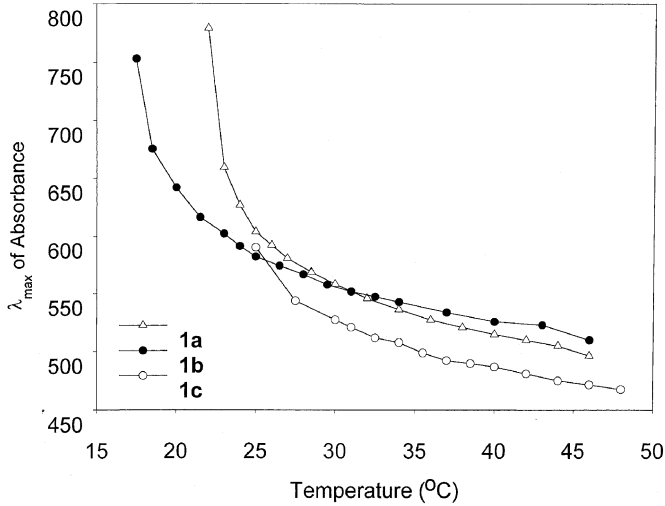

FIGURE 3 Dependence of the preferred wavelength of reflection (λ_{max} in nm) of solid cholesteric films of **1a**–**c** with increase in Temperature (T in °C). Thickness of the films of **1a**–**c** was maintained at 10 μm.

drawing the films carefully in one direction. Figure 3 shows the temperature dependence of λ_{max} for oriented films of **1a**–**c**. The curves consist of two regions, one where the change in λ_{max} with temperature is high ($T < 25°C$) and the other where the change in λ_{max} is small ($T > 25°C$). Such temperature dependencies are characteristic of cholesteric mesophases with underlying smectic A (Sm_A) phase [17]. A notable point in the preparation of cholesteric films is the orientation of the cholesteric phase in the planar texture. Mesophases of **1a**–**c** orient well and show sharp absorbance of light at a given temperature. Reflectivity was nearly 50% (not shown), which is in agreement with the theoretically predicted value for cholesteric structures [18]. For films of **1a**, bandwidths of the wavelength of selective reflection at half height ($\Delta\lambda_{1/2}$) were found to increase from ~30 nm at higher temperature (43°C) to ~60 nm at lower temperatures (17°C). **1b** and **1c** showed identical trends of $\Delta\lambda_{1/2}$, though the variations in $\Delta\lambda_{1/2}$ were within ±4 nm. This suggests that the birefringence, Δn (where $\Delta\lambda_{1/2} = p\Delta n$) for compounds **1a**–**c** are similar. However, the data also revealed that the range of λ_{max} spanned by **1a**–**c** in their mesophase regimes differed. Thus **1a** shows selective reflection spanning a range of 496–779 nm while **1b** shows a range of 510–753 nm. **1c** shows a range of 467–590 nm. It is evident that the range of the λ_{max} spanned by **1a**–**c** is controlled by the nature of the halogen atom in these systems.

Although the nature of the halogen atom in this system does not induce significant variations in the LC textures[2] there are differences in their thermal properties as revealed from differential scanning calorimetry (DSC). **1a**–**c** show cholesteric phase with planar texture at room temperature. The DSC of a precooled (0°C for 48 h) solid mass of **1b** (DSC, Calorimetry Sciences Corporation), upon heating showed a peak at 39.8°C ($\Delta H = 20.9$ kJ/mol) corresponding to the solid to cholesteric phase transition followed by a small transition due to the cholesteric to isotropic liquid transition at 46.5°C ($\Delta H = 0.42$ kJ/mol) (Table 1). Cooling showed no change in the nature of the isotropic to mesophase transition, but the mesophase to solid transition was much reduced in enthalpy ($\Delta H = 0.42$ kJ/mol) and occurred at 16.1°C. The second heating scan showed the solid-to-liquid crystalline transition at 16.7°C which had $\Delta H = 0.42$ kJ/mol and no change in the mesophase-isotropic phase transition. **1a** and **1c** showed similar behavior where, upon heating, the solid-mesophase transition occurred at 39.2 and 41.1°C followed by a mesophase-isotropic liquid transition at 45.3 and 49.5°C, respectively, for the first heating scan. Subsequent heating scans showed the appearance of the cholesteric phase at 22.8 and 24.2°C, respectively, while the clearing temperature remained identical to the first scan for all compounds. All cooling scans for **1a**–**c** were identical. The enthalpies of transition of mesophase to isotropic liquid for **1a**–**c** was in the range of 0.42–1.26 kJ/mol, which is characteristic of the cholesteric mesophase. The thermal data revealed the existence of a Sm_A phase for compounds **1a**–**c**. Importantly, the solid-to-mesophase transition of the first scans of **1a**–**c** showed an increase in enthalpy with progressive increase in size of the halogen atom (Table 1). Coincidentally, the range of wavelength spanned by **1a**–**c** shows a decrease (283, 243, and 123 nm for **1a**, **1b**, and **1c**, respectively) with an increase in the size of the halogen atom. Thus it was evident that these two properties were dependent on the size of the halogen atom.

In order to gain more information on these systems, two more compounds were synthesized, one where the oxygen atom of the ethoxyethylene segment in **1b** was replaced by a methylene group as in **2a**, and the other where the length of polymethylene segment in **2a** was increased as in **2b**. The crystal structures of these two compounds revealed some important information [19].

1. Crystal structure of **2a** at 130 K showed that adjacent molecules were arranged in a head-to-tail fashion and packed to form stacked monolayers (Figure 4). The bromine atom in **2a** is the single atom that makes the largest number (9) of extremely short interatomic contacts, revealing the mode in which the halogen atom stabilizes the solid/crystalline phase in these systems.

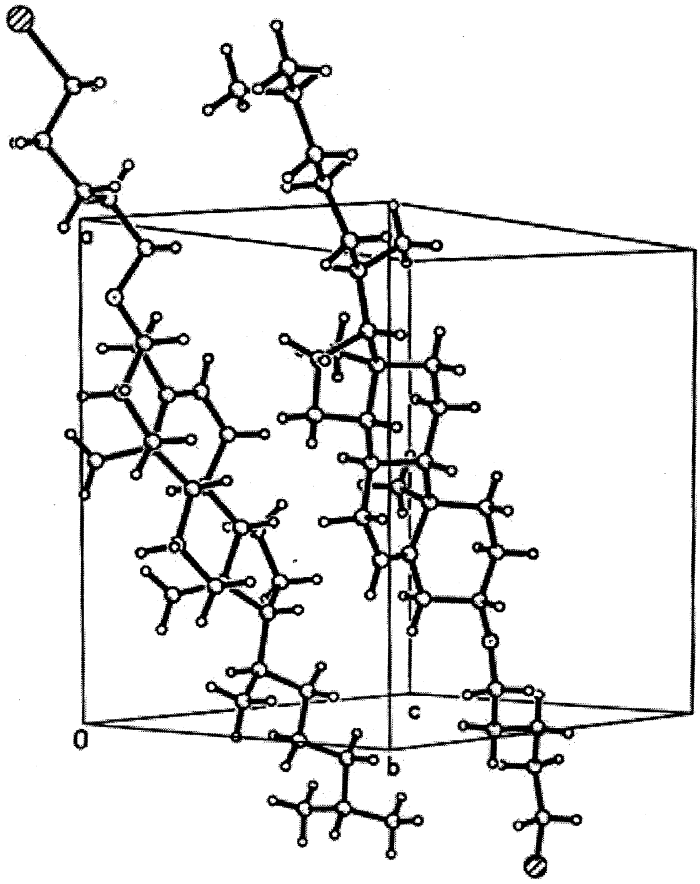

FIGURE 4 Unit cell packing of **2a** at 130 K. Note the closely packed head-to-tail arrangement of adjacent molecules that arrange to form monolayers in the crystalline state.

2. At 298 K, although the polymethylene side chain displayed thermal motion the cholesteryl backbone and the bromine atom could be clearly located, showing their resistance to thermal motion. The cholesteryl backbone is known to behave as a rigid body [20], while the bromine atom, due to its large size and large number of contacts, is able to effectively resist thermal motion.
3. When the length of polymethylene segment was increased, despite the good quality of crystals of **2b**, even at 130 K, the crystal structure could not be determined completely. However, the bromine atom and the cholesteryl backbone could be nicely resolved, indicating that this is due

to thermal motion of the undecamethyl segment and not static disorder in the crystal.

Examination of their LC behavior showed that **2a**–**b** indeed display cholesteric mesophases with platelet type of texture, albeit at higher temperatures that were also thermally characterized (Table 1). From a comparison of the molecular structures of **1b** and **2a**, it is evident that the nature of the side chain governs both the mesophase temperature regimes and the mesophase texture. Interestingly in **2b**, the mesophase was metastable and correspondingly showed inseparable dual peaks in the DSC thermogram. It is evident that these compounds display LC activity due to the flexibility of the side chains, and therefore we reasoned that due to the excessive flexibility of the undecamethylene chain in **2b** (as evidenced from single crystal studies) [19] the resultant mesophase in **2b** is metastable. Though the side chain is susceptible to thermal motion, the halogen atom, due to its large size and strong interatomic contacts (stabilizing interactions in the crystal) offers resistance to this motion. Correspondingly, DSC shows that the solid-to-mesophase transition increases in enthalpy with increase in halogen atom size. This is possibly due to the fact that a larger halogen atom is able to invoke a larger number of stabilizing interatomic contacts in the crystalline phase.

To our knowledge this is structurally one of the simplest nonpolymeric single-component systems displaying a cholesteric phase at room temperature. These compounds offer a useful starting point for a new generation of chemically stable monomeric, as well as polymeric, liquid crystals based on ether derivatives of cholesterol. Commonly used derivatives of cholesterol to this data have been based on carbonyl linkages that are susceptible to hydrolysis. In this context we believe that ether derivatives hold much promise for further applications [21]. We are now investigating a detailed structure-property relationship by exploring more compounds of modified molecular structures to understand the origin of the manifestation of cholesteric mesophases at reduced temperatures.

END NOTES

[1]Compounds **1a**–**c** were synthesized by refluxing cholesterol tosylate (1.00 g) with the corresponding 2-haloethoxyethanol in dry dioxane for 4–6 h. The solvent was removed, the residue partitioned between water and $CHCl_3$ and dried over anhydrous Na_2SO_4. The organic layer was evaporated and the residue purified by column chromatography on silica gel 60–120 mesh using 1:19 EtOAc/Hexane. (**1a**): Iridescent melt, 82%. IR ($CHCl_3$, cm^{-1}): 3370, 2930, 2865, 1465, and 1350. ^1H NMR ($CDCl_3$,

300 MHz); δ: 0.67 (s, 3H), 0.86–2.35 (m, 41H), 3.15 (m, 1H), 3.62 (t, $J = 4.5$Hz, 2H), 3.65 (s, 4H), 3.76 (t, $J = 4.5$ Hz, 2H), 5.28 (d, $J = 4.5$ Hz, 1H). MALDI-TOF: 518 ($M^+ + 2 + Na$), 516 ($M^+ + Na$). Anal. Calcd. for $C_{31}H_{53}O_2Cl$: C, 75.49; H, 10.83; Found: C, 75.9; H, 11.14. (**1b**): iridescent melt, 76%. IR ($CHCl_3$, cm^{-1}): 3370, 2930, 2865, 1465, and 1350. ^{1}H NMR ($CDCl_3$, 300 MHz); δ: 0.67 (s, 3H), 0.86–2.35 (m, 41H), 3.15 (m, 1H), 3.43 (t, $J = 4.5$ Hz, 2H), 3.65 (t, $J = 4.5$ Hz, 4H), 3.76 (t, $J = 4.5$ Hz, 2H), 5.28 (d, $J = 4.5$ Hz, 1H). LR-MS: 538 ($M^+ + 2$), 536 (M^+). Anal. Calcd. for $C_{31}H_{53}O_2Br$: C, 69.25; H, 9.94; Found: C, 69.29; H, 10.26. (**1c**): Iridescent melt, 68%. IR ($CHCl_3$, cm^{-1}): 3370, 2930, 2865, 1465, and 1350. ^{1}H NMR ($CDCl_3$, 300 MHz); δ: 0.67 (s, 3H), 0.86–2.35 (m, 41H), 3.15 (m, 1H), 3.23 (t, $J = 4.5$ Hz, 2H), 3.60 (s, 4H), 3.76 (t, $J = 4.5$ Hz, 2H), 5.28 (d, $J = 4.5$ Hz, 1H). MALDI-TOF: 622 ($M^+ + K + 2$), 620 ($M^+ + K$). Anal. Calcd. for $C_{31}H_{53}O_2I$: C, 63.68; H, 9.14; Found: C, 63.89; H, 9.06. Chemical characterization of compounds **2a**–**b** has been published [16].

[2]Mesophase textures and ranges were observed using a polarizing microscope (Leitz Laborlux 12 POL model) equipped with a Mettler FP 80 temperature controller attached to a hot stage Mettler FP 82 and a CCD camera (Nikon).

Differential scanning calorimetry was carried out on a Calorimetric Sciences Corp. differential scanning calorimeter at a heating rate of 0.5 K/min. All data were analyzed on Origin 6.1 Software.

REFERENCES

[1] (a) Chandrasekhar, S. (1992). *Liquid Crystals*. New York: Cambridge Univ. Press, pp. 213–299.
(b) de Gennes, P. G., & Prost, P. (1993). *The Physics of Liquid Crystals*, New York: Oxford University Press, pp. 263–266.

[2] (a) Hikmet, R. A. M., & Lub, J. (1996). *Prog. Polym. Sci.*, *21*, 1165.
(b) Freemantle, M. (1996). *Chem. Eng. News*, *74*, 33.
(c) Müller, M., Zentel, R., & Keller, H. (1997). *Adv. Mater.*, *9*, 159.
(d) Broer, D. J., Lub, J., & Mol, G. N. (1995). *Nature*, *378*, 467.

[3] Schadt, M., & Helfrich, W. (1971). *Appl. Phys. Lett.*, *18*, 127.

[4] (a) Schaeffer, T. J., & Nehring, J. (1984). *Appl. Phys. Lett.*, *45*, 1021.
(b) Schadt, M., Buchecker, R., & Müller, K. (1989). *Liquid Crystals*, *5*, 293.

[5] Schadt, M. (1997). *Annu. Rev. Mater. Sci.*, *27*, 305–379.

[6] (a) Crawford, G. P., & Zumer, S. (1996). (Eds.), *Liquid Crystals in Complex Geometries* London: Taylor & Francis.
(b) Kitzerow, H. S. (1994). *Liquid Crystals*, *16*, 1–31.

[7] Kricheldorf, H. R. (1999). *Adv. Polym. Sci.*, *141*, 83–188.

[8] Hikmet, R. A. M. (1990). *J. Appl. Phys.*, *68*, 4406.

[9] Hikmet, R. A. M., & Kemperman, H. (1998). *Nature*, *392*, 476–479.

[10] (a) Hou, H. Q., Reuning, A., Wendorff, J. H., & Greiner, A. (2000). *Macromol. Chem. Physic.*, *201*, 2050–2054.

(b) Godinho, M. H., Costa, C., & Figueirinhas, J. L. (1999). *Mol. Cryst. Liq. Cryst.*, *331*, 2033–2039.

[11] (a) He, G.-X., Wada, K., Kikukawa, T., & Matsuda, T. (1987). *Chem. Commun.*, 1294.
(b) Gokel, G. W., Hernandez, J. C., Viscariello, A. M., Arnold, K. A., Champan, C. F., Echegoyen, L., Frorczek, Gandour, R. D., Morgan, C. R., Trafton, J. E., Miller, S. R., Minganti, C., Eiband, D., Schulz, R. A., & Tamminen, M. (1987). *J. Org. Chem.*, *52*, 2963.
(c) Tamaoki, N., Parfenov, A. V., Masaki, A., & Matsuda, H. (1997). *Adv. Mater.*, *9*, 157.
(d) Ledder, B. (1971). *J. Chem. Phys.*, *54*, 4671.
(e) Hölter, D., Frey, H., Mülhaupt, R., & Klee, J. E. (1998). *Adv. Mater.*, *10*, 864.
(f) Hoyle, C. E., Watanabe, T., & Whitehead, J. B., (1994). *Macromolecules*, *27*, 6581.

[12] (a) Shinkai, S., Shimamoto, K., & Manabe, K. (1989). *Makromol. Chem. Rapid Commun.*, *10*, 361.
(b) Mahler, W., & Panar, M. (1972). *J. Am. Chem. Soc.*, *94*, 7195.
(c) Chistyakov, I., & Kosterin, E. A. (1964). *Rost. Kristallov.*, *4*, 68.
(d) Cholesteryl oleate is also known to form a monotropic liquid crystal upon cooling from 44°C.

[13] Yang, D.-K., Huang, X.-Y., & Zhu, Y.-M. (1997). *Annu. Rev. Mater. Sci.*, *27*, 117–146.

[14] Mc. Donnell, G. G., & Gray, G. W. (Eds.), (1987). *Thermotropic Liquid Crystals*, *22*, 120–144.

[15] Sage, I., & Bahadur, B. (Eds.), (1990). *Liquid Crystals-Applications and Uses*, *3*, 302–344.

[16] (a) Krishnan-Ghosh, Y., Visweswariah, S. S., & Bhattacharya, S. (2000). *FEBS Lett.*, *473*, 341.
(b) Bhattacharya, S., & Krishnan-Ghosh, Y. (2001). *Langmuir*, *17*, 2067.

[17] The smectic-A (Sm_A) phase has an infinitely long pitch. When the temperature is decreased towards the n*- Sm_A transition the temporal Sm_A structure that develops on a small scale causes the pitch to increase dramatically with decrease in temperature. Therefore with decrease in temperature, the reflected light changes from blue to red. Tsutui, T., & Tanaka, R., (1980). *Polymer*, *21*, 1351.

[18] Fergason, J. L. (1966). *Mol. Cryst.*, *1*, 293.

[19] Krishnan-Ghosh, Y., Gopalan, R. S., Kulkarni, G. U., & Bhattacharya, S. (2001). *J. Mol. Struct.*, *560*, 345.

[20] Schomaker, V., & Trueblood, K. N. (1968). *Acta Cryst.*, *B24*, 63.

[21] (a) Eskenazi, C., Nicoud, J. F., & Kagan, H.B. (1979). *J. Org. Chem.*, *44*, 995.
(b) Leigh, W. J., & Mitchell, D. S. (1988). *J. Am. Chem. Soc.*, *110*, 1311.
(c)Weiss, R. G. (1988). *Tetrahedron*, *110*, 3413.
(d) Shinkai, S., Nishi, T., Ikeda, A., Matsuda, T., Shimamoto, K., & Manabe, O. (1990). *Chem. Commun.*, 303.